Journal of Alloys and Compounds 509 (2011) 6616–6620

Contents lists available at ScienceDirect

Journal of Alloys and Compounds

journal homepage: www.elsevier.com/locate/jallcom

A simple thermal decomposition–nitridation route to nanocrystalline boron nitride (BN) from a single N and B source precursor

Hong Zhang[a], Youjian Chen[a], Jianhua Ma[a,b,*], Hanxuan Tong[c], Jiang Yang[c], Danwei Ni[c], Huiming Hu[c], Fangqing Zheng[c]

[a] College of Chemistry and Materials Engineering, Wenzhou University, Wenzhou, Zhejiang 325027, PR China
[b] Nanomaterials and Chemistry Key Laboratory, Advanced Materials Research Center of Wenzhou, Wenzhou University, Wenzhou, Zhejiang 325027, PR China
[c] Oujiang College, Wenzhou University, Wenzhou, Zhejiang 325027, PR China

ARTICLE INFO

Article history:
Received 30 November 2010
Received in revised form 16 March 2011
Accepted 17 March 2011
Available online 29 March 2011

Keywords:
Boron nitride
Chemical synthesis
X-ray diffraction
HRTEM
Thermogravimetric analysis

ABSTRACT

Nanocrystalline boron nitride (BN) was synthesized via a simple thermal decomposition–nitridation route by the reaction of hydrated ammonium tetraborate ($NH_4HB_4O_7{\cdot}3H_2O$) and metallic magnesium powders in an autoclave at 650 °C. The crystal phase, morphology, grain size, and chemical composition of the as-prepared products were characterized in detail by X-ray powder diffraction (XRD), energy dispersion spectroscopy (EDS), X-ray photoelectron spectroscopy (XPS), field-emission scanning electron microscopy (SEM), transmission electron microscopy (TEM), and high-resolution transmission electron microscopy (HRTEM). The products were also studied by FT-IR and the thermogravimetric analysis (TGA). Results revealed that the as-synthesized nanocrystalline were h-BN, and they had diameters within 100 nm. They had good thermal stability and oxidation resistance in high temperature.

1. Introduction

Boron nitride (BN) has attracted intense interest due to its many unique physical and chemical properties, such as low density, high temperature stability, high thermal conductivity, high melting point, low dielectric constant and chemical inertness. Owing to these properties, boron nitride can be used as lubricants, electrical insulators, refractory and so forth [1–5].

Boron nitride (BN) has several different phases: such as cubic (c-BN), hexagonal (h-BN), wurtzite (w-BN), and rhombohedral (r-BN) etc. [6–8]. Among them, h-BN has a similar carbon graphite-like structure. In hexagonal structure, the interlayer interactions are weak (van der Waals type) and the intralayer interactions are strong (covalent B–N bonds (sp2)) [9]. So boron nitride (BN) is often referred to as "white graphite" [10].

Traditionally, many approaches have been developed for preparation of BN, such as the direct reaction of boron and nitrogen [11], and the carbothermic reduction of boric oxide [12]. In addition, other methods have also been developed to prepare BN [13–16]. Recently, some new methods have been used to synthesize boron nitride. Ma et al. [10] prepared nanocrystalline boron nitride by the reaction of $NaBH_4$ and NaN_3 in an autoclave at 600 °C. Li et al. [17] reported that hexagonal BN (h-BN) particles were prepared by using BBr_3, NH_4Br and metallic Na as reactants in stainless steel autoclaves at 450 °C for 24 h. Zhang et al. [9] prepared high-purity and bulk-quantity boron nitride spheres at 1400 °C via a simple polymer-chemical route.

In this paper, we use $NH_4HB_4O_7{\cdot}3H_2O$ as boron source and nitrogen source, metallic Mg powders as reductant. Nanocrystalline hexagonal boron nitride has been synthesized via a simple thermal decomposition–nitridation route by the reaction of hydrated ammonium tetraborate ($NH_4HB_4O_7{\cdot}3H_2O$) with metallic Mg powders in an autoclave at 650 °C for 8 h. Compared to the previous methods, this simple route has the primary advantage, i.e., B and N sources from a single cheap safe precursor $NH_4HB_4O_7{\cdot}3H_2O$.

2. Experimental

All of the manipulations were carried out in a dry glove box with flowing nitrogen gas. In a typical experiment, 0.02 mol (about 4.57 g) analytical grade $NH_4HB_4O_7{\cdot}3H_2O$ and 0.11 mol (about 2.64 g) analytical grade metallic Mg powders were put into a mortar, followed by mixing these powders thoroughly. Then the mixture was put into a stainless steel autoclave. After sealing under argon atmosphere, the autoclave was heated at 650 °C for 8 h, followed by cooling to room temperature in the furnace. The obtained product from the autoclave was washed several times with absolute ethanol, dilute HCl aqueous solution, distilled water to remove the impurities. Finally the product was washed three times with absolute ethanol to remove water. The final product was vacuum-dried at 60 °C for 12 h. White powders were obtained.

* Corresponding author at: College of Chemistry and Materials Engineering, Wenzhou University, Wenzhou, Zhejiang 325027, PR China. Tel.: +86 577 86669317; fax: +86 577 86689508.
E-mail address: mjh820@ustc.edu (J. Ma).

0925-8388/$ – see front matter © 2011 Elsevier B.V. All rights reserved.
doi:10.1016/j.jallcom.2011.03.109

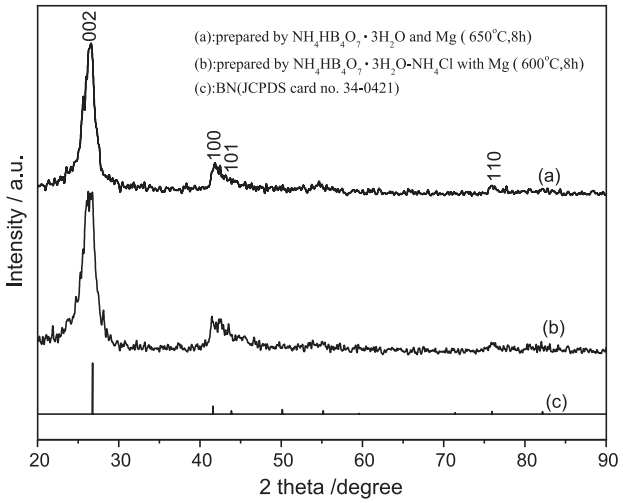

Fig. 1. XRD patterns of the as-prepared samples and standard pattern.

The obtained sample was analyzed by powder X-ray diffraction (XRD) on a Bruker D8 Advance X-ray powder diffractometer using Cu K-α radiation (wavelength λ = 1.54178 Å) and X-ray photoelectron spectra (XPS) analysis was performed on a AXIS ULTRA DLD X-ray photoelectron spectrometer, using Monochrome Al Ka as the excitation source. The morphology of the sample was examined on a JEOL JSM-6700F scanning electron microscope at an accelerating voltage of 10 kV. Energy dispersive spectrometry (EDS) analysis of the product was carried out on an OXFORD INCA instrument attached to the scanning electron microscopy in the scanning range of 0–20 kV. The microstructure and morphologies of the samples were also obtained from transmission electron microscopy (TEM) images and high-resolution TEM (HRTEM) images were recorded on a FEI Tecnai F-20 transmission electron microscopy at an acceleration voltage of 200 kV. Fourier transformation infrared spectroscopy (FT-IR) spectra were obtained using a Shimadzu IR-400 spectrometer by using pressed KBr disks. The thermogravimetric analysis was performed on a thermal analyzer (Model: Q600) below 1000 °C in air at a rate of 10 °C min^{-1} to study its thermal stability and oxidation behavior. All the measurements were carried out at room temperature.

3. Results and discussion

3.1. X-ray diffraction

Fig. 1 shows the XRD patterns of the as-prepared samples and the standard pattern of BN. The pattern (a) is about the product prepared by the reaction of $NH_4HB_4O_7 \cdot 3H_2O$ and Mg powders under 650 °C and 8 h. In the pattern (a), there are four obvious diffraction peaks on this pattern. And all these diffraction peaks ((0 0 2), (1 0 0), (1 0 1) and (1 1 0)) at different *d*-space can be indexed as hexagonal boron nitride (BN). The refinement gives the cell constants (a = 2.504 Å, c = 6.668 Å), which is consistent with the value reported in the literature (a = 2.504 Å, c = 6.656 Å) (JCPDS card no. 34-0421). No evidences of impurities such as B, B_2O_3, other boron nitrides, can be found in this XRD patterns. It should be noted that the disappearance of some weak peaks (such as 50.149° 2-theta and 55.164° 2-theta) existing in standard h-BN spectra may indicate the imperfect crystallization of the final product. The discrepancy between the observed and the theoretical peak positions is most probably caused by the defects and the curvature of the layered structure [9].

3.2. Scanning electron microscopy

The morphology of the prepared BN samples was investigated by field emission scanning electron microscopy. Fig. 2(a) and (b) shows typical SEM images of the BN sample. They reveal that the BN sample consists of particles within 100 nm in diameters. These particles exhibit slightly agglomerated particle morphology due to the ultrafine size of the sample.

3.3. EDS spectrum and XPS spectra

The EDS spectrum in Fig. 3 further demonstrates that the product prepared at 650 °C for 8 h is composed of nearly stoichiometric B and N (the atomic ratio of B to N was estimated to be 46.48:53.52), without the contamination of oxygen.

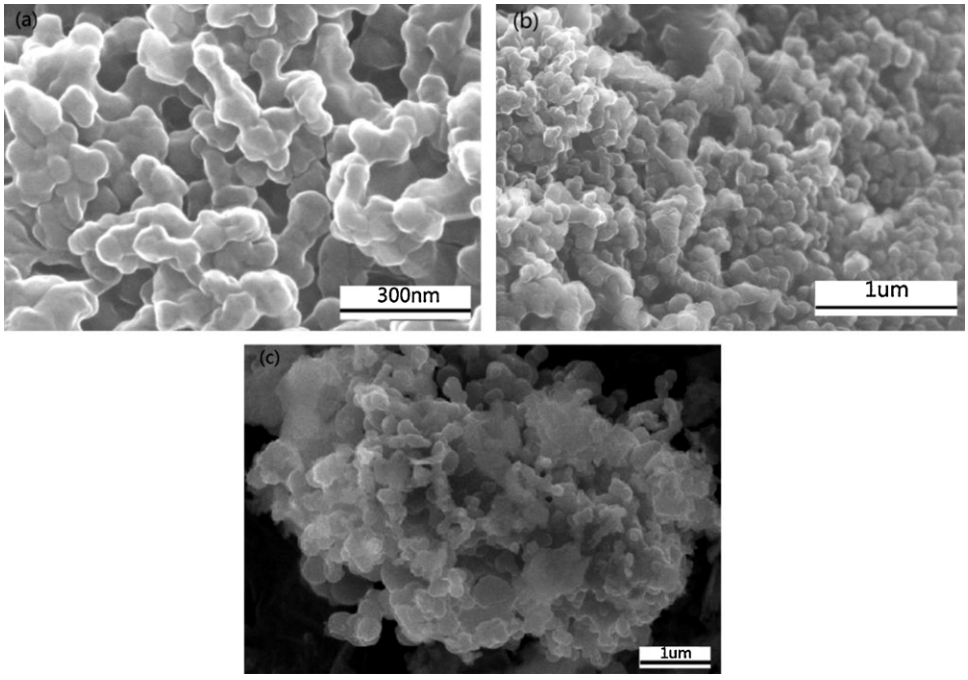

Fig. 2. SEM images of the as-prepared BN samples.

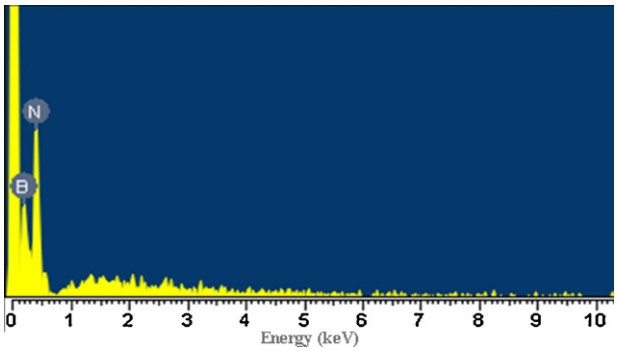

Fig. 3. EDS spectrum of the as-prepared h-BN sample.

The composition and purity of the as-synthesized BN nanoparticles are further investigated by XPS. Fig. 4 shows the results of the XPS spectra. They show that the sample surface consists of nitrogen, boron, carbon and oxygen, with binding energies of N 1s, B 1s, C 1s and O 1s at 395.5, 190.89, 281.95 and 529.85 eV, respectively. The C 1s and O 1s peaks indicate that there exists a small amount of impurity elements such as C and O due to the adsorption of CO_2, H_2O and O_2 on the surface of the sample. The B 1s peak at 190.89 eV and the N 1s peak at 395.5 eV indicate BN, in good agreement with those in the literature [18]. The quantification of B 1s and N 1s peaks confirmed that the atomic ratio of B:N was 1.07:1, which closely agrees with the stoichiometric composition of BN. This result is consistent with the XRD and EDS pattern presented above.

3.4. TEM images and SAED pattern

The morphologies and microstructures of BN were further investigated by TEM and SAED. Fig. 5(a) shows a typical TEM image of the prepared BN superstructures.

The image shows that it consists of particles that have an average diameter of 100 nm.

The particle is further confirmed by the HRTEM image presented in Fig. 5(b). As shown in the image, the adjacent lattice fringes have score break, which are in accord with the analysis of the XRD pattern presented above. The SAED pattern of BN samples is Fig. 5(c). In this pattern, two obvious diffraction rings can be found. These rings can be indexed as (0 0 2) and (1 0 0). And the SAED pattern of the sample can also confirm the crystallinity of BN, in which the diffraction ring diameters again correspond well to the hexagonal BN structure.

3.5. FT-IR spectra

Fig. 6 shows the FT-IR spectra of the particle BN sample at room temperature. Two strong peaks around 1385 and 795 cm^{-1} could be observed clearly for the sample, which are assigned to the B–N stretching vibrations and B–N–B bending vibrations, respectively [19,20]. A weak peak around 3421 cm^{-1} could be attributed to the moisture absorbed on the surface of the sample.

3.6. Thermogravimetric analysis

To investigate the thermal stability and the oxidation resistance of the as-prepared nanocrystalline BN, A typical TGA/DTA was carried out at temperatures below 1000 °C under flowing air. Fig. 7 shows the TGA/DTA curves of the sample. From the TGA curve, we can find that the weight of the product has not changed significantly below 900 °C except a slight water weight loss on the surface. But the quantity of the adsorbed water is very small. As the temperature keeps on rising from 900 °C to 950 °C, there is an obvious weight

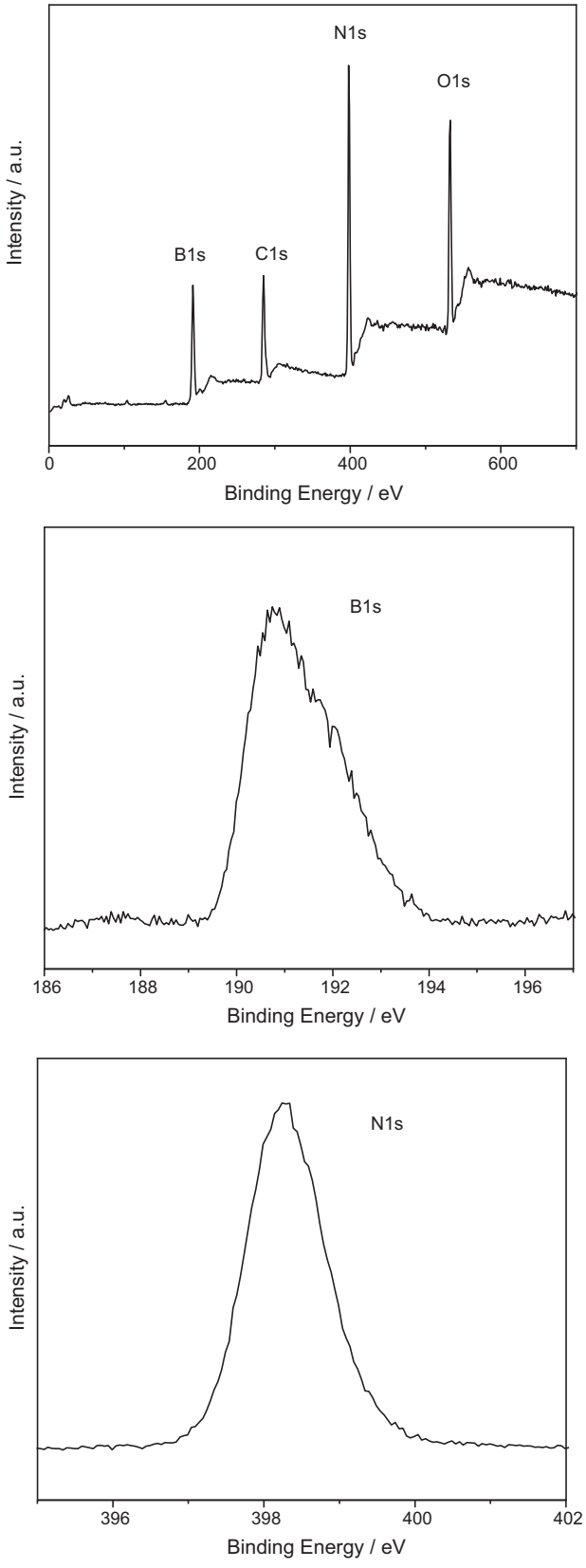

Fig. 4. XPS survey spectrum of the as-prepared h-BN sample.

gain during the process, indicating that the BN sample is oxidized into B_2O_3 and nitrogen oxides. This can also be confirmed by the DTA curve of the sample, shown in the Fig. 7. In this DTA curve, there is a big exothermic peak at 940 °C relative to the extensive oxidation of the sample. Around 1000 °C B_2O_3 is evaporating exten-

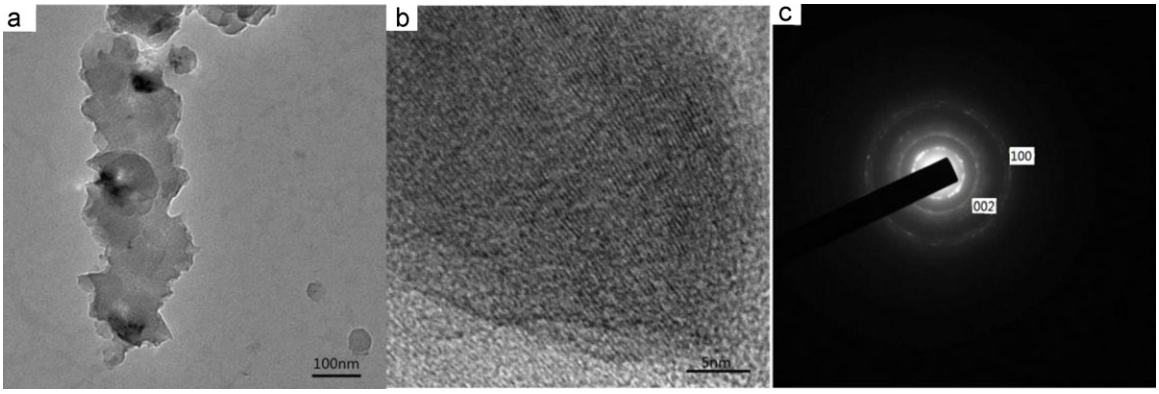

Fig. 5. (a) TEM image, (b) HRTEM image and (c) SAED pattern of the as-prepared h-BN sample.

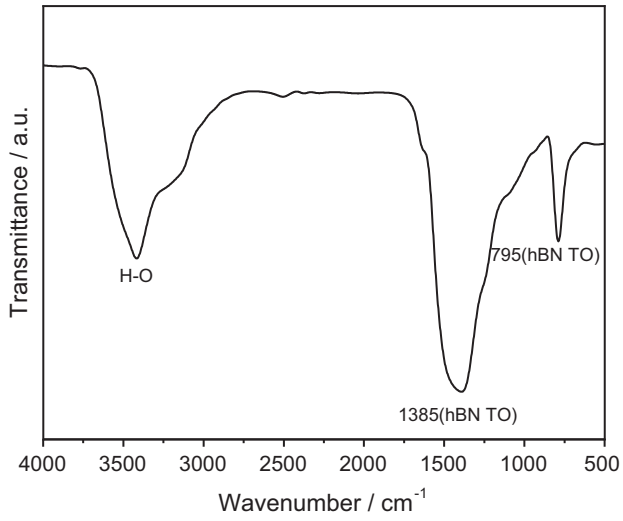

Fig. 6. FT-IR spectra of the BN sample.

sively [21], which counteracts the weight gain due to the oxidation of BN, so the weight levels off. Thus, B_2O_3 evaporation results in the final weight gain less than the theoretical one (41.67%) [22]. These indicate that the prepared BN has good thermal stability and anti-oxidation property under 900 °C.

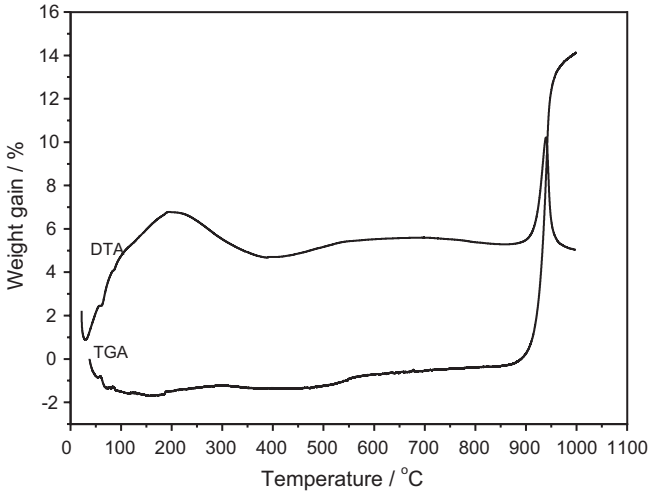

Fig. 7. TGA/DTA curves heated in flowing air for the BN sample.

In our experiments, as the temperature rose, $NH_4HB_4O_7{\cdot}3H_2O$ could decompose generating NH_3 and H_2O gases and B_2O_3. So the pressure in the autoclave may be very high. At the reaction temperature, B_2O_3, NH_3 and metallic magnesium powders could react with each other to produce BN. The high pressure in the autoclave would be helpful for reducing the reaction temperature and enhancing the reaction speed. The produced H_2O gas could react with Mg powders producing H_2 gas. Therefore, the possible thermal decomposition–nitridation route might be expressed as follows:

$$NH_4HB_4O_7{\cdot}3H_2O \rightarrow NH_3 + 2B_2O_3 + 4H_2O \quad (1)$$

$$B_2O_3 + 3Mg \rightarrow 2B* + 3MgO \quad (2)$$

$$2H_2O + Mg \rightarrow Mg(OH)_2 + H_2 \quad (3)$$

$$Mg(OH)_2 \rightarrow MgO + H_2O \quad (4)$$

$$2B* + 2NH_3 \rightarrow 2BN + 3H_2 \quad (5)$$

And the total reaction process can be represented as the following:

$$2NH_4HB_4O_7{\cdot}3H_2O + 11Mg = 2BN + 11MgO + 3B_2O_3 + 11H_2 \quad (6)$$

In the reaction, the prepared B_2O_3 would react with H_2O into HBO_2 or H_3BO_3. HBO_2 (or H_3BO_3) and MgO would be removed through HCl aqueous solution and distilled water. The final product was nanocrystalline BN.

In this route, the B source has not made the most of utility. In order to make the full use of the B source, we optimize the synthesis method, i.e. NH_4Cl as other N source. BN can also be produced by the reaction of 0.01 mol $NH_4HB_4O_7{\cdot}3H_2O$, 0.12 mol Mg powders and 0.03 mol NH_4Cl in an autoclave at 600 °C for 8 h. Fig. 1(b) is the XRD pattern of the as-prepared sample with new route, it shows that the product is also hexagonal BN. Fig. 2(c) is the SEM image of the new route BN sample, it can be observed that the sample mainly consists of particles within 100 nm in diameters.

4. Conclusion

In summary, nanocrystalline BN has been prepared via a simple thermal decomposition–nitridation route by the reaction of hydrated ammonium tetraborate ($NH_4HB_4O_7{\cdot}3H_2O$) with metallic Mg powders in an autoclave at 650 °C for 8 h. The product has the nanocrystalline h-BN structure, it consists of particles within 100 nm in diameters, and the product has good thermal stability and oxidation resistance below 900 °C.

Acknowledgments

This work was supported by Innovation and Promotion of Science-Technology Project of Zhejiang Province and the

Department of Education of Zhejiang Province of China under Grant No. 20070546.

References

[1] T.K. Paul, P. Bhattacharya, D.N. Bose, Appl. Phys. Lett. 56 (1990) 2648.
[2] L. Liu, Y.P. Feng, Z.X. Shen, Phys. Rev. B 68 (2003) 104102.
[3] K. Watanabe, T. Taniguchi, H. Kanda, Nat. Mater. 3 (2004) 404.
[4] H. Mass, A. Currao, G. Calzaferri, Angew. Chem. Int. Ed. 41 (2002) 2495.
[5] L. Shi, Y.L. Gu, Y.T. Qian, et al., Mater. Lett. 58 (2004) 3301.
[6] A.V. Kurdyumov, V.L. Solozhenko, W.B. Zelyavski, J. Appl. Cryst. 28 (1995) 540.
[7] R.-F. Liu, C. Cheng, Phys. Rev. B 76 (2007) 014405.
[8] V.L. Solozhenko, D. Hausermann, M. Mezouar, M. Kunz, Appl. Phys. Lett. 72 (1998) 1691.
[9] T. Zhang, G. Wen, L. Xia, et al., Scripta Mater. 63 (2010) 415.
[10] J.H. Ma, J. Li, G.X. Li, et al., Mater. Res. Bull. 42 (2007) 982.
[11] J.B. Condon, C.E. Holcombe, D.H. Johnson, L.M. Steckel, Inorg. Chem. 15 (1976) 2173.
[12] K.A. Schwetz, A. Lipp, in: W. Gerhartz, al. et (Eds.), Ulmann's Encylopedia of Industrial Chemistry, vol. 4, VCH, Weinheim, 1985, p. 295.
[13] M.Y. Yu, S.Y. Dong, D.L. Cui, et al., J. Cryst. Growth 270 (2004) 85.
[14] M.Y. Yu, K. Li, D.L. Cui, et al., J. Cryst. Growth 269 (2004) 570.
[15] X.P. Hao, D.L. Cui, G.X. Shi, et al., Mater. Lett. 51 (2001) 509.
[16] L.Y. Chen, M.X. Huang, Y.T. Qian, et al., Mater. Lett. 58 (2004) 3634.
[17] M.H. Li, L.Q. Xu, Y.T. Qian, et al., Diamond Relat. Mater. 18 (2009) 1421.
[18] C.D. Wagner, W.M. Riggs, L.E. Davis, et al., Handbook of X-ray Photoelectron Spectroscopy, 55344, Perkin–Elmer Corporation, Eden Prairie Minn, 1979.
[19] V. Cholet, L. Vandenbulcke, J.P. Rouan, et al., J. Mater. Sci. 29 (1994) 1417.
[20] S. Sadananda, K. Stefan, I. Lubica, et al., J. Eur. Ceram. Soc. 18 (1998) 1037.
[21] A. Tampieri, A. Bellosi, J. Mater. Sci. 28 (1993) 649.
[22] L.Y. Chen, Y.L. Gu, Y.T. Qian, Mater. Res. Bull. 39 (2004) 609.